Original paper

S100A16 cooperates with DEPDC1 to promote the progression and angiogenesis of nephroblastoma through PI3K/Akt/mTOR pathway

Geng Geng[1], Yongtao Xu[1], Qingfang Li[1], Qinghao Li[1], Lili Yuan[2], Mengyao Dong[3], Ming Ming[1]

[1]Department of Pediatric Surgery, The Affiliated Taian City Central Hospital of Qingdao University, Taian, Shandong, P.R. China
[2]Department of Administration, The Affiliated Taian City Central Hospital of Qingdao University, Taian, Shandong, P.R. China
[3]Department of Neonatal Intensive Care Unit, The Affiliated Taian City Central Hospital of Qingdao University, Taian, Shandong, P.R. China

S100 calcium-binding protein A16 (S100A16) has previously been reported to play a role in tumor cells. Nevertheless, the role that S100A16 played in nephroblastoma cells remains obscure.

The expression of S100A16 and DEPDC1 were detected via RT-q PCR and western blotting. Cell transfection was performed to overexpress DEPDC1 or interfere S100A16. CCK8 was applied for the assessment of cell viability. The apoptotic level and the capabilities of WiT49 cells to proliferate, invade and migrated were appraised utilizing Tunel, colony formation Transwell, and wound healing, separately. The angiogenesis was estimated through tube formation assay. Co-immunoprecipitation (CO-IP) was performed to examine the targeted binding of S100A16 to DEPDC1. The contents of PI3K/Akt/mTOR pathway-related proteins were resolved by virtue of western blot.

S100A16 and DEPDC1 expression levels were significantly increased in nephroblastoma cell lines. S100A16 deletion suppressed nephroblastoma cell proliferative, invasive, migrative and angiogenetic capabilities but facilitated the apoptotic level. Moreover, S100A16 could bind DEPDC1, DEPDC1 overexpression partially reversed the inhibitory effect of S100A16 interference on nephroblastoma cell. DEPDC1 overexpression also partially counteracted the suppressive impacts of S100A16 interference on PI3K/Akt/mTOR pathway-related proteins.

S100A16 synergistic with DEPDC1 promotes the progression and angiogenesis of nephroblastoma cell through the PI3K/Akt/mTOR pathway.

Key words: nephroblastoma, DEPDC1, S100A16, angiogenesis, PI3K/Akt/mTOR pathway.

Introduction

Nephroblastoma (Wilms tumor – WT), which is an aggressive malignant cancer, especially happens in children under the age of 5 years of age, accounting for 90% of childhood renal tumors and constitutes 7% of all childhood malignancies [1]. Due to lacking obvious early symptom, the majority of nephroblastoma

patients are diagnosed with advanced stage [2]. With advancements in medical care, radical resection, as well as chemoradiotherapy, the overall 5-year survival rate has reached 90% in high-income countries [3]. However, there remains 15% of children die due to recurrence, metastasis and insensitivity to chemotherapy drugs [4]. In this way, the exploration of hidden molecular basis mechanisms and the development of new therapeutic strategies for the management of nephroblastoma patients are of great necessity.

The S100 family, which has abundant existence in different organs and tissues, is a kind of calcium-binding proteins and consists of over 20 members [5]. S100 proteins serve as key intracellular Ca^{2+} sensors and extracellular factors that participate in multiply basic processes, like cell proliferation, tissue repair, as well as cell apoptosis [6]. Being a novel part of S100 protein family, S100 calcium-binding protein A16 (S100A16) is closely related to chromosomal rearrangements and instability [7]. S100A16 acts as a critical player in various signaling pathways, such as Notch, as well as nuclear factor kappa B pathways, the dysregulation of which is also observed in various tumor cells [8]. S100A16 overexpression contributes to gastric cancer cell invasive and migrative capabilities [9]. S100A16 causes pancreatic cancer cells to proliferate and migrate via AKT and ERK1/2 signaling pathway [10]. Additionally, zhu et.al also proved that S100A16 promotes the progression prostate cancer through activating cell signaling proteins AKT and ERK [11]. All of the above studies suggest that S100A16 may serve as a novel therapeutic or diagnostic target in human cancers. However, the effect of the S100A16 in nephroblastoma is yet to be fully elucidated.

Through analyzing the BioGRID database, we found that S100A16 could bind with DEP domain containing 1 (DEPDC1). However, the complex association between S100A16 and DEPDC1 in the cell proliferation and tumor growth has not yet been studied. DEPDC1 is a highly conserved gene that participate in multiple cellular processes, like cell proliferation, cell apoptosis, along with signaling transduction [12]. DEPDC1 is a novel oncoantigen that has abundant existence in various malignancies, including bladder cancer [13], hepatocellular carcinoma [14] and colorectal cancer [15], which may act as a vital diagnostic hallmark as well as a therapeutic target for human cancers. A recent study found that DEPDC1 is upregulated in nephroblastoma, which has close association with poor patient survival [16]. In our previous study, we also found that DEPDC1 expression is significantly increased in nephroblastoma cell that promotes the malignant progression of nephroblastoma, while DEPDC1 interference suppressed the capabilities of nephroblastoma cells to proliferate and invade [17]. These results indicating that DEPDC1 may act as an early molecular marker for nephroblastoma, nevertheless, the biological function and mechanism of DEPDC1 in nephroblastoma are still obscure. An increasing number of reports have demonstrated that the phosphatidylinositol 3-kinase (PI3K)/Akt/mammalian target of rapamycin (mTOR) signaling pathway is closely connected with tumorigenesis [18, 19]. Notably, Zhao *et al.* found that DEPDC1 participates in the hyper-activation of PI3K/AKT/mTOR signaling, resulting in breast cancer advancement and poor survival [20].

In this study, we explored the clinical significance and functional implication of S100A16 in nephroblastoma. Moreover, we also investigate the relation between S100A16 and DEPDC1 in the cell proliferation and poor prognosis of nephroblastoma and the underlying molecular mechanism regrading PI3K/AKT/mTOR axis.

Material and methods

Cell culture and treatment

Human normal renal cell line (HK-2), nephroblastoma cell lines (WiT49, 17-94 and GHINK-1) and human umbilical vein endothelial cells (HUVECs) that provided by The American Type Culture Collection got cultivated in DMEM (Hyclone; Cytiva) which was decorated with 10% (Hyclone; Cytiva), and 1% antibiotics (Beyotime Institute of Biotechnology) at 37°C with 5% CO_2.

Cell Counting Kit-8 (CCK-8) assay

CCK-8 assay was utilized for the estimation of cell viability. Briefly, the inoculation of WiT49 cells in a 96-well cell culture plate was implemented, after which was the overnight cultivation at 37°C with 5% CO_2. Subsequently, 10 μl CCK-8 solution (cat. no. P0037; Beyotime) was put into per well to further cultivate the cells for 4 h. The OD value was decided in the precise of λ= 450 nm by means of a microplate reader (BioTek Instruments, Inc.).

Cell transfection

Initially, the injection of WiT49 cells (3×10^5 cells/well) in 6-well plates was implemented, after which was 24 h of cultivation at 37°C with 5% CO_2. Subsequently, S100A16-targeting short hairpin (sh) RNA (sh-S100A16#1, sh-S100A16#2, and sh-NC) and the overexpression-DEPDC1 (Ov-DEPDC1) vector and the NC empty vector (Ov-NC) that provided by Shanghai GenePharma Co., Ltd were transfected into WiT49 cells at a concentration of 25 nM by virtue of Lipofectamine® 2000 in light of standard protocol. Cells in blank control group received no transfection. After 48 h, the transfection efficiency was detected using reverse transcription-quantitative PCR (RT-qPCR) and western blotting.

Colony formation assay

The inoculation of WiT49 cells, which were suspended (5×10^2 cells/well) in DMEM, into 6-well plates was carried out, following which was 14 d of cultivation at 37˚C. Afterwards, WiT49 cells were subjected to 15 min of 70% ethanol fixation and 20 min of 0.05% crystal violet staining. Finally, the number of colonies formed was totaled (≥ 50 cells/colony) utilizing an Olympus GX53 light microscope (Olympus Corporation; magnification, ×4).

Wound healing

The injection of WiT49 cells in 6-well plates (1×10^5 cells/well) was operated. When 70-80% cell fusion was achieved, the medium was replaced with serum-free DMEM and the cells were incubated overnight at 37˚C at 5% CO_2. Subsequently, a 200-μl sterile pipette tip was used to scratch the cell monolayer. afterwards, the PBS-rinsed cells were cultivated at 37˚C with 5% CO_2. Images were collected at 0 and 24 h by means of a BX51 inverted microscope (magnification, ×100). The area of wound closure in each picture was determined by using ImageJ software (version. 1.52; National Institutes of Health). The calculation of migration rate was implemented based on the following formula: % migration = scratch current width / scratch original width × 100.

Transwell

The capability of WiT49 cells to invade was assessed utilizing Transwell chambers (BD Biosciences) with Matrigel pretreatment. Briefly, Matrigel (BD Biosciences) was employed for the pretreatment of 24-well Transwell plates (Corning, Inc.) with 8-μm pore inserts at 37˚C for 30 min. Next, 4×10^4 cells were placed in plasma-free medium. The upper chamber was precoated with matrix (Sigma-Aldrich; Merck KGaA) and cells were cultured in the upper chamber with 0.1 ml cell suspension/well, whereas cell culture medium that contained 20% FBS was injected into the lower chamber. Subsequently, the invading cells were subjected to 4% formaldehyde fixation and 0.3% crystal violet solution (Sigma-Aldrich; Merck KGaA) staining. The observation of invading cells in five randomly selected fields was operated under an inverted microscope (magnification, ×100). The calculation of invasion rate was operated based on the following formula: % invasion = invaded cells in lower chamber/total cells added to top chamber ×100.

TUNEL assay

Apoptosis was appraised utilizing One Step TUNEL Apoptosis Assay Kit (Beyotime Institute of Biotechnology) in light of standard protocol. Briefly, the WiT49 cells were washed with PBS three times and then fixed at room temperature (20-25˚C) with 4% paraformaldehyde (Beyotime Institute of Biotechnology) for 15 min. Then, the exposure of cells to 0.15% Triton-X-100 was operated for further 5 min. Terminal deoxynucleotidyl transferase solution and FITC-deoxyuridine triphosphate solution (Roche Diagnostics GmbH) were added to the cells and the cells were incubated at 37˚C for 60 min in the dark. The staining of nuclei was conducted with DAPI (0.5 μg/ml). Antifade Mounting Medium was used to seal the cells. Cells were randomly selected from 5 fields of view and an inverted fluorescence microscope (Olympus Corporation) was used to observe excitation and emission wavelengths within the range of 450-500 and 515-565 nm (green fluorescence), respectively. Apoptosis index = number of apoptotic cells/(number of apoptotic cells + normal cells).

Tube formation assay

24-well culture plate, 200 μl pipette tips and matrigel matrix glue were placed at 4˚C overnight. Subsequently, about 200 μl of matrix gel was sucked into the 24-well plate, and kept in a cell incubator to gel for 30 min. Before that, the culture medium of WiT49 in each group (Control CM, sh-NC CM, sh-S100A16 CM, sh-S100A16 + Oe-NC CM and sh-S100A16 + Oe-DEPDC1 CM) was changed to serum-free culture medium for 24 h. Then, the digestion of cells was implemented by means of trypsin-EDTA solution (Beyotime, cat. no. C0201) to prepare a single-cell solution. The culture medium that decorated with 300 μl serum and 10 μl single cell suspension was added to each well. Finally, photographs were captured under the help of an inverted microscope (ZEISS, Axio Vert. A1, magnification, ×40).

Co-immunoprecipitation (Co-IP) assay

The quantification of total proteins, which were isolated from WiT49 cells utilizing RIPA lysis buffer (Beyotime Biotechnology, Inc.), was implemented by means of BCA kits (Beyotime Biotechnology, Inc.). For immunoprecipitation, the overnight cultivation of 400 μg proteins with 2 μg antibodies was carried out at 4°C. Subsequently, the addition of 30 μl Protein G/A agarose beads (Invitrogen) was operated and cell lysates got cultivated for 3 h. Following the rinse with PBS, the precipitated protein was resuspended in 5 × SDS-PAGE loading buffer, boiled for 5 min, and eluted from the beads. Finally, immunoblotting was used to detect the immunoprecipitation products.

Western blotting

The quantification of total proteins, which were isolated from WiT49 cells utilizing RIPA lysis buffer, was implemented by virtue of a BCA Protein Assay

Kit. Following denaturation in a 95°C metal bath, SDS-PAGE was performed with a 12% gel for 20 μg protein samples. The transferring of separated proteins to PVDF membranes was implemented. Subsequently, the overnight cultivation of membranes, which were impeded by 5% skimmed milk, with primary antibodies specific to DEPDC1 (dilution, 1:1,000; cat. no. ab184182; Abcam), S100A16 (dilution, 1:1,000; cat. no. ab130419; Abcam), Bcl-2 (dilution, 1:1,000; cat. no. ab194583; Abcam), Bax (dilution, 1:1,000; cat. no. ab32503; Abcam), phosphorylated (p)-PI3K (dilution, 1:500; cat. no. ab154598; Abcam), p-Akt (dilution, 1:1,000; cat. no. ab38449; Abcam), PI3K (dilution, 1:1,000; cat. no. ab191606; Abcam), Akt (dilution, 1:1,000; cat. no. ab8805; Abcam), p-mTOR (dilution, 1:1,000;

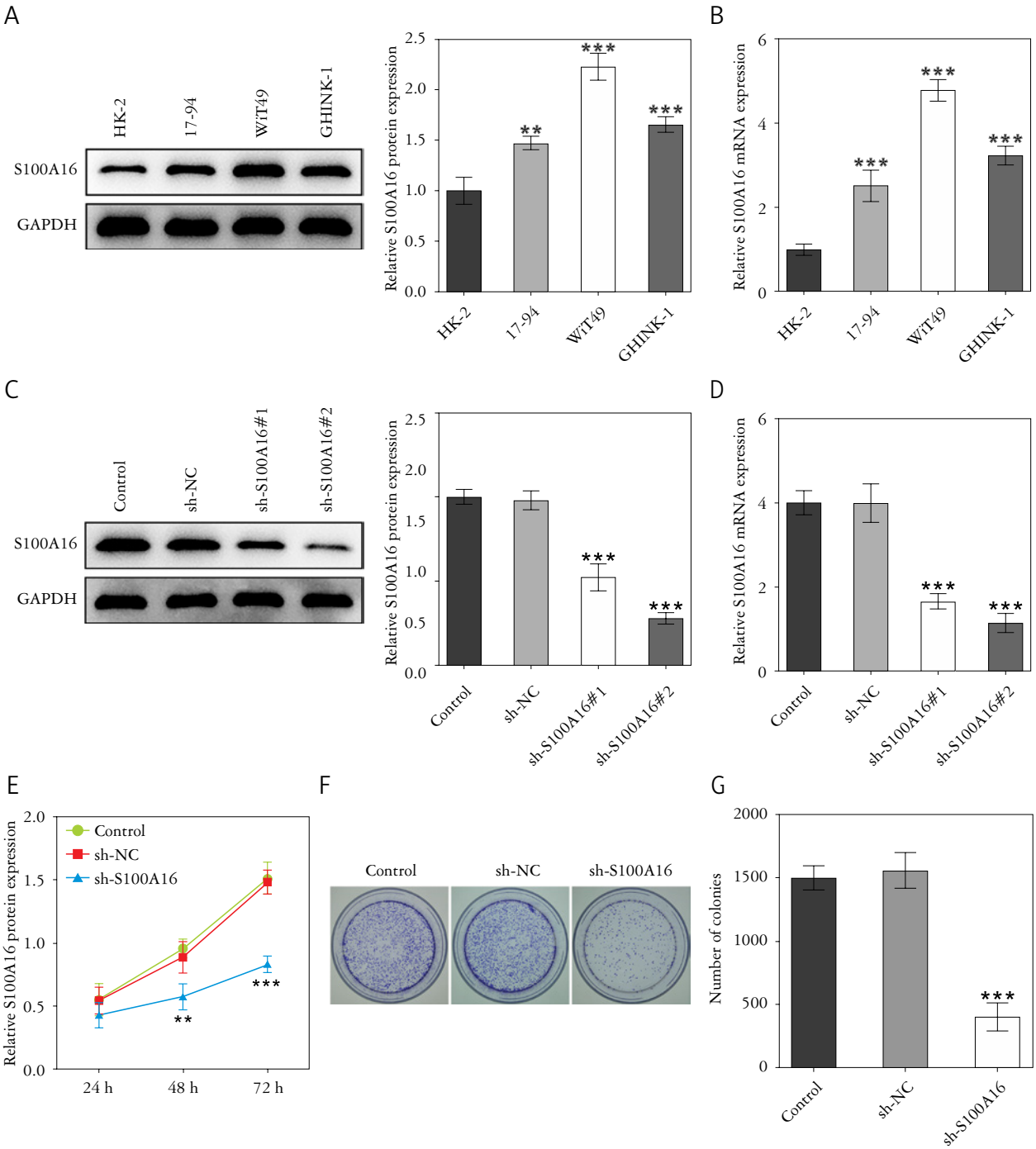

Fig. 1. Interference with S100A16 suppressed the proliferation of nephroblastoma cells. The expression of S100A16 in nephroblastoma cell lines was detected by **A**) western blot and **B**) RT-qPCR, respectively. Interference efficiency of S100A16 was detected via **C**) western blot and **D**) RT-qPCR. **E**) CCK-8 was used to detect the level of cell proliferation. **F**) Cloning experiment was used to detect the cell cloning level; $^{**}p < 0.01$ and $^{***}p < 0.001$ vs. HK-2 or sh-NC

cat. no. Ab109268; Abcam), mTOR (dilution, 1:5,000; cat. no. Ab32028; Abcam) and GAPDH (dilution, 1:1,000; cat. no. ab181602; Abcam) was operated at 4˚C, after which was the exposure to goat anti-rabbit HRP-binding IgG secondary antibody (dilution, 1:5,000; cat. no. ab6721; Abcam) for 1 h. The determination of protein bands was carried out utilizing ECL reagent (MilliporeSigma). Bands were semi-quantified and normalized using ImageJ v1.46 software (National Institutes of Health).

RT-qPCR

The quantification of RNA, which was extracted from sample cells with RNAzol RT (Sigma-Aldrich; Merck KGaA), was operated with the adoption of a NanoDrop spectrophotometer (Thermo Fisher Scientific, Inc.). Following DNase I digestion, the transcription of RNA into cDNA was performed through a QuantiTect Reverse Transcription kit (Qiagen GmbH) in light of standard protocol. With the help of a QuantiTect SYBR Green PCR kit (Qiagen GmbH), qPCR was operated in light of suggested protocol. The following were the sequences of primers (GenScript): DEPDC1 forward 5'-TCTGCCATGAAGTGCCTAGC-3', reverse 5'-TGATGTAGCCACAAACAACCAAA-3'; S100A16 forward 5'-CACAAGTGGCCAACGGAAAG-3', reverse 5'-GCTGGCGGGGCCTAAG-3' or GAPDH forward 5'-AGCCACATCGCTCAGACAC-3', reverse 5'-GCCCAATACGACCAAATCC-3'. The relative mRNA expression levels was appraised with comparative Ct method.

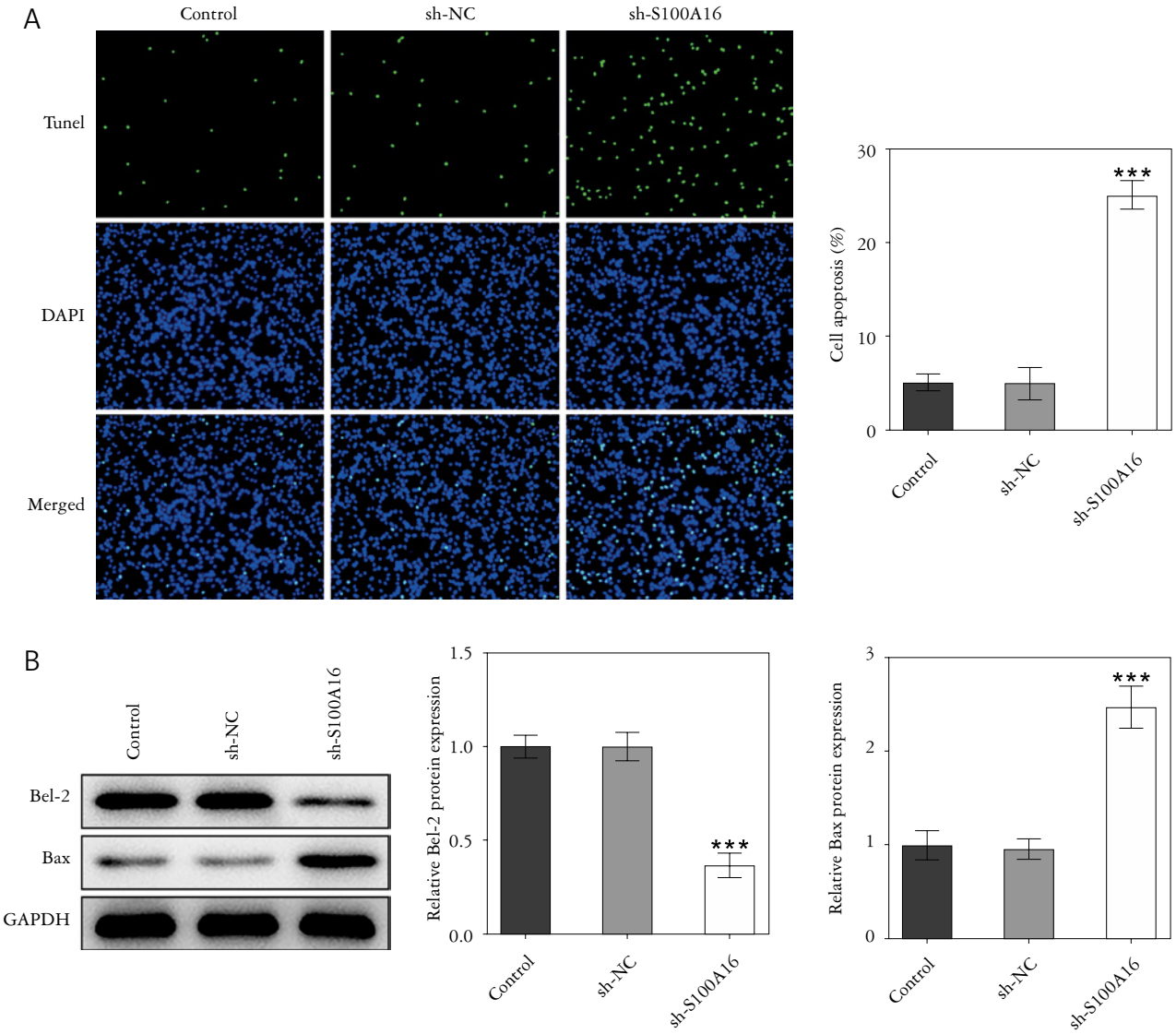

Fig. 2. Interference of S100A16 induced apoptosis of nephroblastoma cells. **A**) Cell apoptosis was detected by Tunel staining. **B**) The expression levels of apoptosis-related proteins (Bax and Bcl-2) were improved by western blot; $^{***}p < 0.001$ vs. sh-NC

Statistical analysis

Data that displayed in the way of mean ± SD got analyzed with GraphPad Prism 8.0.2 software (GraphPad Software, Inc.). Statistical differences were determined using a one-way ANOVA followed by Tukey's post hoc test for group comparisons. P-value less than 0.05 was supposed to demonstrate statistically significant difference.

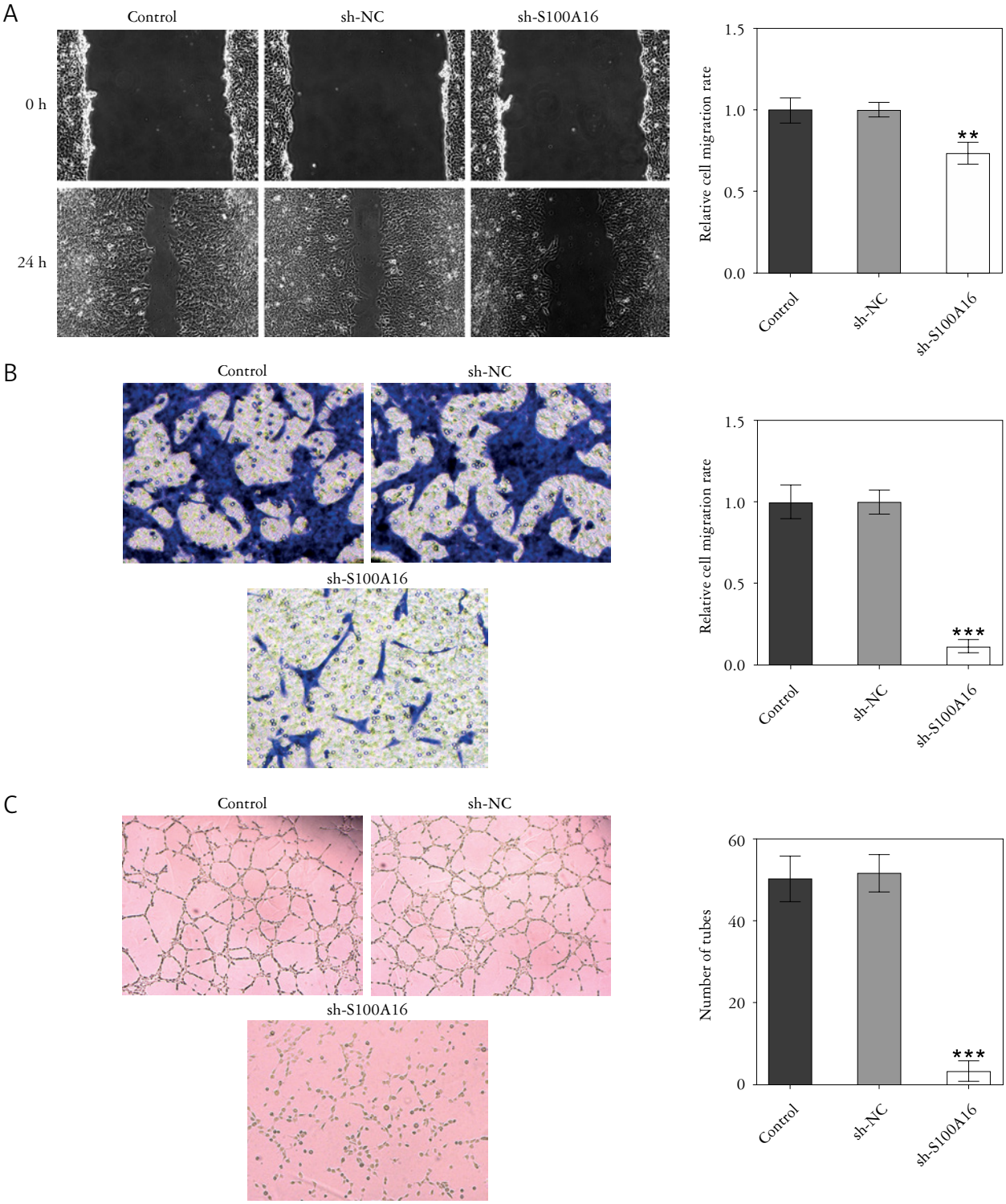

Fig. 3. S100A16 knockdown inhibited invasion, migration and angiogenesis of nephroblastoma cells. **A**) Wound healing and **B**) Transwell were used to detect the level of migration and invasion of WiT49 cells. **C**) Tubule formation assay was used to detect the tubule formation ability of HUVEC cells; $^{**}p < 0.01$ and $^{***}p < 0.001$ vs. sh-NC

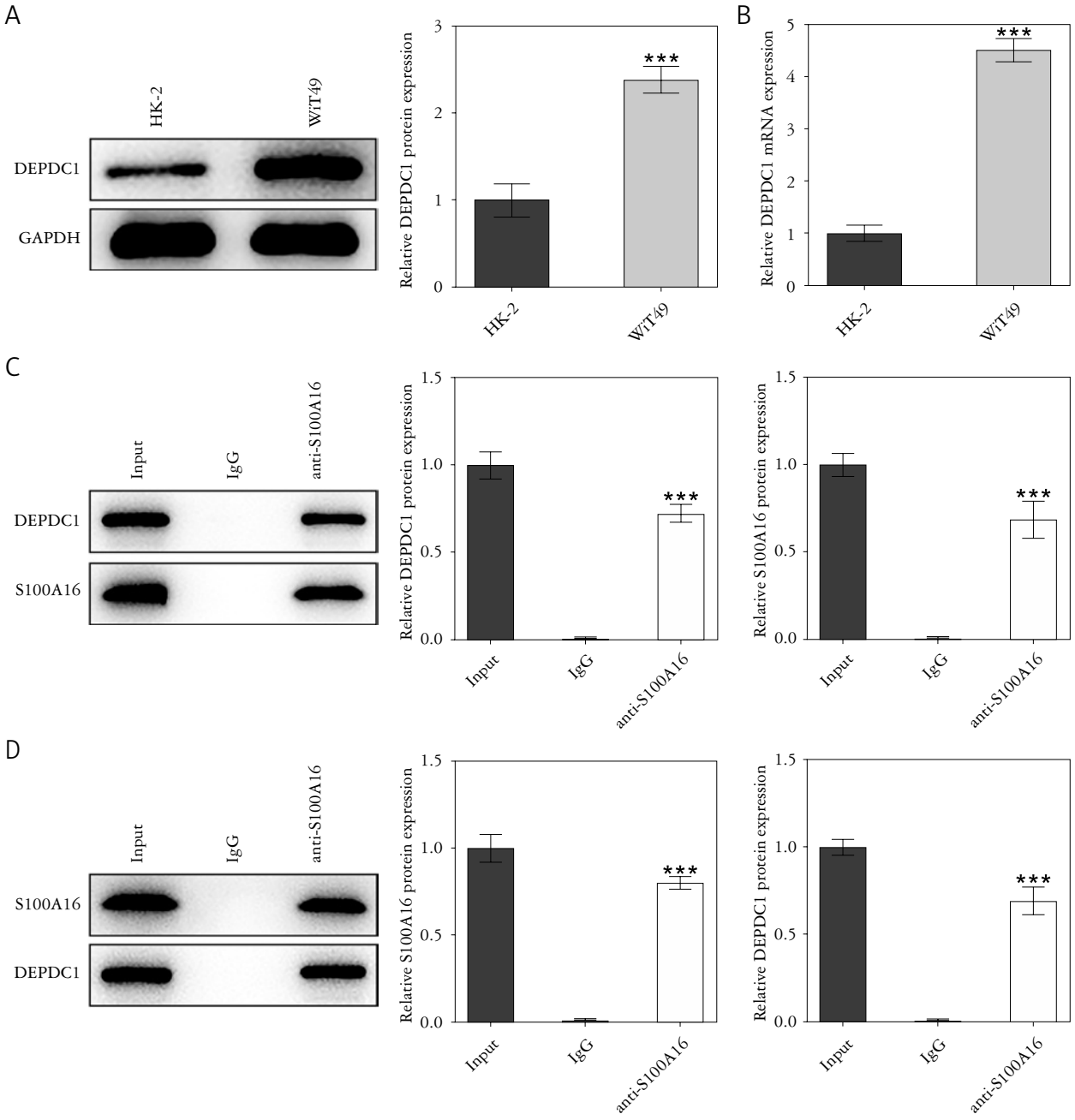

Fig. 4. DEPDC1 is highly expressed in nephroblastoma cells and interacts with S100A16. **A)** Western blot and **B**) RT-qPCR were performed to detect the expression of DEPDC1 in nephroblastoma cells. **C-D**) Co-immunoprecipitation assay was used to detect the targeted binding of S100A16 to DEPDC1; $^{***}p < 0.001$ vs. HK-2 or IgG

Results

Interference with S100A16 suppressed the proliferation of nephroblastoma cells

Western blot (Fig. 1A) and RT-qPCR (Fig. 1B) were employed for the estimation of S100A16 expression at both mRNA and protein levels in nephroblastoma cell lines. It was discovered that compared with that in HK-2 cells, S100A16 was got an elevation in WiT49, 17-94 and GHINK-1. It was noted that S100A16 had the highest expression in WiT49 cells. In view of this, WiT49 cells were adopted for the following experiment. By constructing the S100A16 interference plasmid, western blot (Fig. 1C) as well as RT-qPCR (Fig. 1D) was applied for the examination of interference efficiency. It was uncovered that S100A16 expression in WiT49 cells was conspicuously reduced after S100A16 interference. Compared with sh-S100A16#1, sh-S100A16#2 had a higher interference efficiency. In this way, sh-S100A16#2 was adopted for ensuing experiments. Results obtained from CCK-8 (Fig. 1E) and clone formation as-

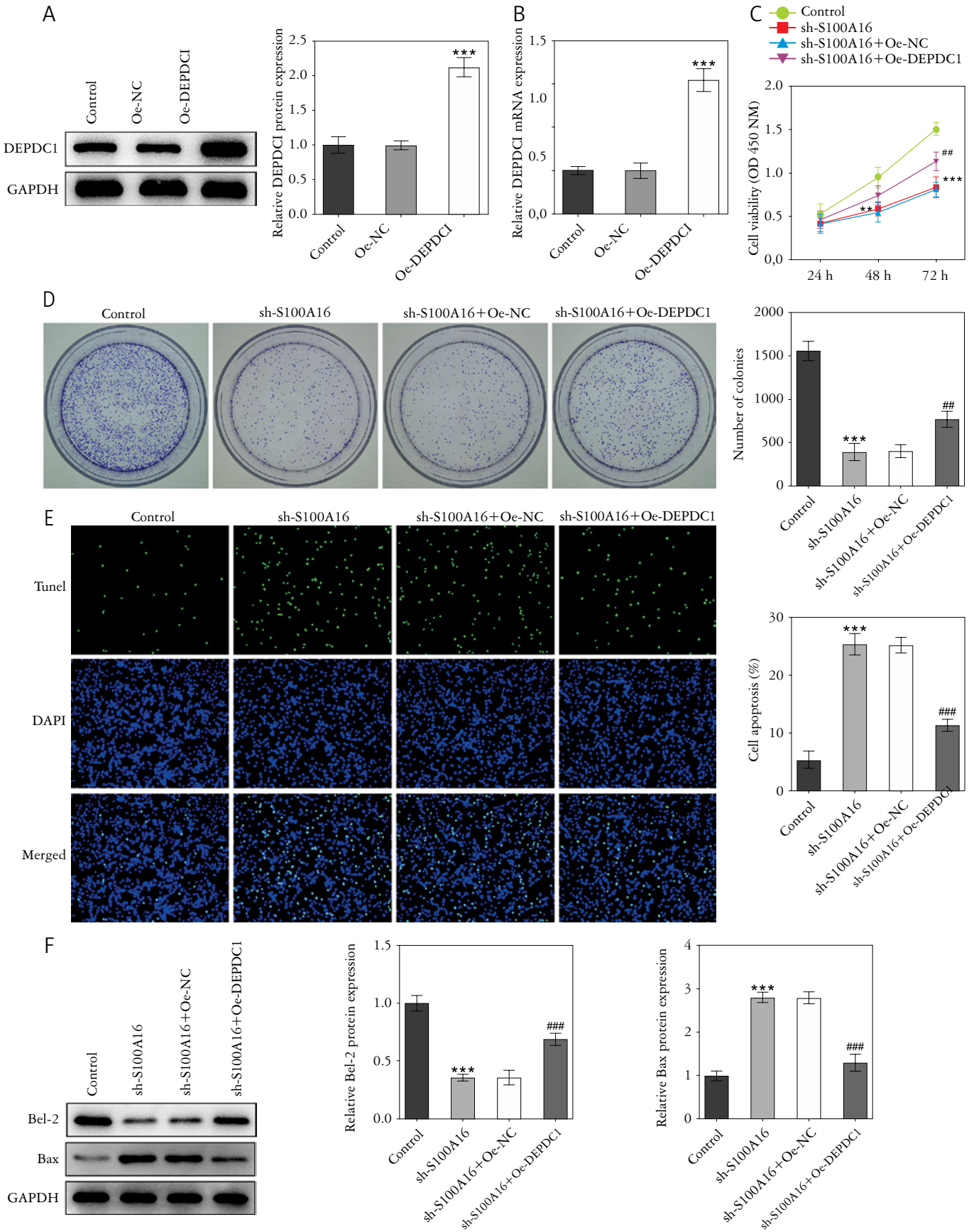

Fig. 5. Upregulation of DEPDC1 partially reversed the effects of S100A16 interference on the proliferation and apoptosis of nephroblastoma cells. Interference efficiency of DEPDC1 was detected via **A**) western blot and **B**) RT-qPCR. **C**) CCK-8 was used to detect the level of cell proliferation. **D**) Cloning experiment was used to detect the cell cloning level. **E**) Cell apoptosis was detected by Tunel staining. **F**) The expression levels of apoptosis-related proteins (Bax and Bcl-2) were detected by western blot; $^{**}p < 0.01$ and $^{***}p < 0.001$ vs. Oe-NC or Control; $^{\#\#}p < 0.01$ and $^{\#\#\#}p < 0.001$ vs. sh-S100A16 + Oe-NC

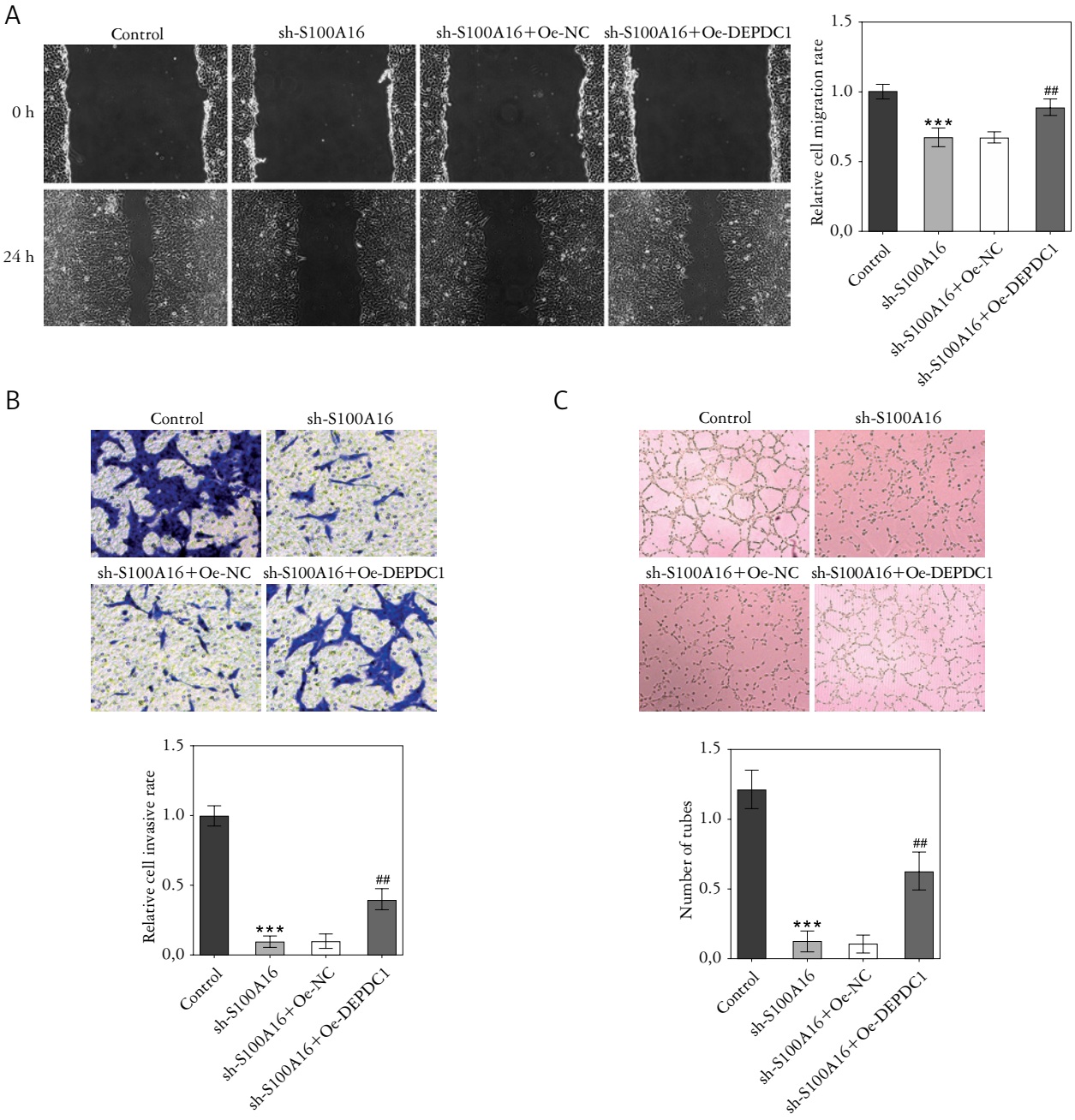

Fig. 6. Upregulation of DEPDC1 partially reversed the inhibitory effect of S100A16 interference on the migration, invasion and angiogenesis of nephroblastoma cells. **A**) Wound healing and **B**) Transwell assays were used to detect cell migration and invasion. **C**) Tubule formation assay was used to detect the tubule formation ability of HUVEC cells; $^{***}p < 0.001$ vs. Control; $^{\#\#}p < 0.01$ vs. sh-S100A16 + Oe-NC

say (Fig. 1F) depicted the impacts of S100A16 interference on WiT49 cell proliferation. Compared with sh-NC group, S100A16 interference significantly reduced cell proliferation.

Interference of S100A16 induced apoptosis of nephroblastoma cells

Figure 2A depicted the effect of S100A16 interference on apoptosis of WiT49 cells. Relative with the sh-NC group, S100A16 interference markedly facilitated the apoptosis rate of WiT49 cells. Results obtained from western blot displayed that (Fig. 2B) interfering S100A16 ascended the contents of Bax but descended the content of Bcl-2, indicating that interfering S100A16 could significantly promote cell apoptosis.

S100A16 knockdown inhibited invasion, migration and angiogenesis of nephroblastoma cells

Wound Healing (Fig. 3A) and Transwell (Fig. 3B) were applied for the appraisement of cell invasive and

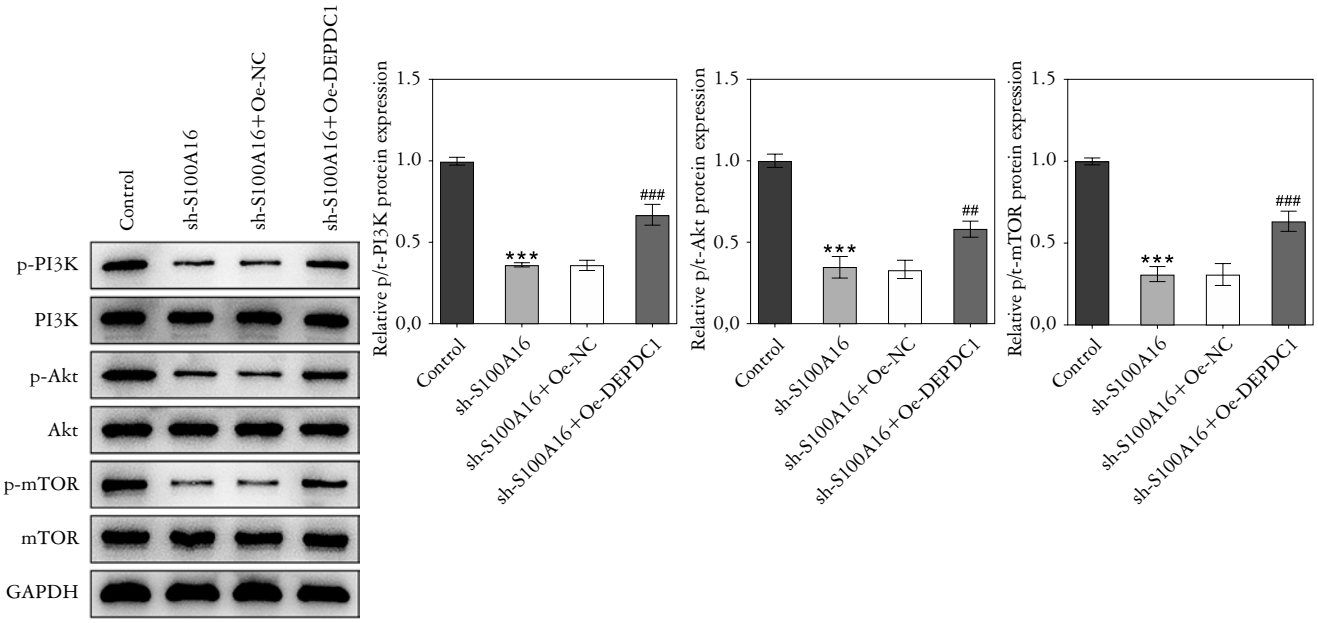

Fig. 7. S100A16 cooperates with DEPDC1 to regulate PI3K/Akt/mTOR pathway. The expressions of p-AKT, AKT, mTOR, p-mTOR, P13K and p-P13K inWiT49 cells were detected by western blot; $^{***}p < 0.001$ vs. Control; $^{\#\#}p < 0.01$ and $^{\#\#\#}$ $p < 0.001$ vs. sh-S100A16 + Oe-NC

migrative capabilities, respectively. By contrast with sh-NC group, sh-S100A16 group significantly inhibited cell invasion and invasion. Subsequently, tubule formation experiment was performed to detect the tubule formation ability of HUVEC cells, which were demonstrated in Fig. 3C. Compared with HUVEC cells cultured in sh-NC conditioned medium, the tubule formation ability of HUVEC cells treated with sh-S100A16 conditioned medium was significantly suppressed. The above results suggest that S100A16 knockdown could inhibit the migrative, invasive and angiogenetic capabilities of nephroblastoma cells.

DEPDC1 is highly expressed in nephroblastoma cells and interacts with S100A16

Western blot (Fig. 4A) and RT-qPCR (Fig. 4B) were applied for the estimation of DEPDC1 at both mRNA and protein levels in nephroblastoma cells. Relative with HK-2 cells, the mRNA and protein expressions of DEPDC1 were remarkably enhanced WiT49 cells. Subsequently, co-immunoprecipitation assay was used to verify the targeted binding of S100A16 and DEPDC1 (Fig. 4C-D). the precipitation experiment with IgG showed that DEPDC1 protein and S100A16 protein were not precipitated, which indicated that DEPDC1 protein and S100A16 protein could not bind to IgG. Notably, we found that both DEPDC1 and S100A16 could be precipitated either by using protein DEPDC1 to precipitate protein S100A16 or by using protein S100A16 to precipitate DEPDC1. These results implied that DEPDC1 could interact with S100A16.

Upregulation of DEPDC1 partially reversed the effects of S100A16 interference on the proliferation and apoptosis of nephroblastoma cells

With the purpose of figuring out the mechanism of DEPDC1 and S100A16 in nephroblastoma cells, DEPDC1 overexpression plasmid was constructed and transfected into WiT49 cells to make DEPDC1 overexpression (Fig. 5A-B). CCK-8 (Fig. 5C) as well as clone formation assay (Fig. 5D) demonstrated that DEPDC1 overexpression greatly promoted cell proliferation compared with sh-S100A16 + Oe-NC group. Tunel staining (Fig. 5E) suggested that DEPDC1overexpression reversed the promoting effect of S100A16 interference on cell apoptosis. Western blot (Fig. 5F) results showed that Bcl-2 protein expression was up-regulated and Bax protein was down-regulated in sh-S100A16 + Oe-DEPDC1 group compared with sh-S100A16 + Oe-NC, which also proved this result.

Upregulation of DEPDC1 partially reversed the inhibitory effect of S100A16 interference on the migration, invasion and angiogenesis of nephroblastoma cells

Wound Healing (Fig. 6A) and Transwell (Fig. 6B) were employed for the assessment of cell invasive and migrative capabilities. It was discovered that DEP-

DC1 overexpression was more conducive to cell invasion and migration than sh-S100A16 + Oe-NC group. Moreover, tubule formation experiment (Fig. 6C) was carried out to detect the tubule formation ability of HUVEC cells and it was revealed that relative with the sh-S100A16 + Oe-NC CM group, sh-S100A16 + OE-DEPDC1 conditioned medium treated-WiT49 cells had enhanced angiogenesis ability. To conclude, DEPDC1 overexpression partially reversed the inhibition of S100A16 interference on cell migration, invasion and angiogenesis.

S100A16 cooperates with DEPDC1 to regulate PI3K/Akt/mTOR pathway

The contents of PI3K/Akt/mTOR pathway-related proteins were appraised via western blot (Fig. 7). Relative with the control group, interference with S100A16 reduced the contents of p-PI3K, p-Akt and p-mTOR. Importantly, relative with sh-S100A16 + Oe-NC group, Overexpression of DEPDC1partially reversed the inhibitory effect of S100A16 interference on PI3K/Akt/mTOR pathway related proteins. These results suggest that S100A16 may synergistically regulate PI3K/Akt/mTOR pathway with DEPDC1. It was further demonstrated that S100A16 and DEPDC1 promoted the progression and angiogenesis of nephroblastoma through the PI3K/Akt/mTOR pathway.

Discussion

Nephroblastoma is the most common childhood abdominal malignancy and approximately 15% of patients will experience recurrence with a 40 to 80% overall survival rate [21]. Although the diagnosis and therapeutic effects have significantly improved, long-term survival rate remains low in patients with nephroblastoma with high mortality rate [22]. Therefore, exploring the effects of factors related to early nephroblastoma could further the understanding of nephroblastoma development and help to develop novel efficient treatment strategies.

The S100 protein family members are structurally similar to each other; however, they are not functionally interchangeable. S100A16 has been reported to be a critical player in a wide range of pathophysiological processes, such as inflammation, adipogenesis, osteoporosis as well as tumor progression [23, 24]. Of note, S100A16 has been speculated to be an essential prognostic marker for numerous tumors, like colorectal cancer [8], pancreatic cancer [25] and non-small cell lung adenocarcinoma [26]. Previous studies have revealed that upregulated S100A16 is closely related to cancer cell differentiation, development and prognosis. However, a recent study suggested S100A16 could serve as a tumor suppressor [27]. Thus, the role that S100A16 played in cancer progression remains obscure. Besides, the effect of S100A16 on the biological activity of nephroblastoma cells remains undetermined. In this study, we investigated whether S100A16 serves a functional role in nephroblastoma progression in vitro. Firstly, we found the expression of S100A16 in nephroblastoma cell WiT49 was significantly increased via RT-qPCR and Western blot analysis, indicating that S100A16 plays a carcinogenic role in nephroblastoma cells that may be a novel prognostic biomarker for nephroblastoma. To further verify this hypothesis, we subsequently constructed S100A16 low expression vectors, and evaluated the proliferative and migrative abilities of WiT49 cells. As expected, silencing S100A16 showed the converse effects. S100A16 depletion remarkably suppressed the capabilities of WiT49 cells to migrate, invade and proliferate. Moreover, down-expression of S100A16 also promoted the apoptosis of WiT49 cells, as evidenced by decreased Bcl-2 level and increased Bax level.

DEPDC1, as a recently identified novel oncogene has been implicated in multiple tumors development and poor clinical outcomes of the patients, like gastric cancer [28], breast cancer [19], lung adenocarcinoma cells [29], along with bladder cancer [30]. The dysregulation of DEPDC1 may promote prostate cancer cell proliferation and the malignant behavior of cancer cells [31]. Nevertheless, the role that DEPDC1 played in nephroblastoma remains elusive. In this study, it was discovered that DEPDC1 was abundant in nephroblastoma cells, which had close association with tumor malignancy and advanced stage. This funding is in line with the results of put forward by Gent *et al*. [17]. Intriguingly, we found that DEPDC1 could combined with S100A16 through the prediction of BioGRID database, suggesting a close relationship between DEPDC1 and S100A16 in nephroblastoma progression. The co-immunoprecipitation test found that DEPDC1 could be combined with S100A16. Further study revealed that overexpression of DEPDC1 reverses the inhibitory effects of sh-RNA-S100A16 on nephroblastoma cells invasion and migration. These results indicate that S100A16 may interact with DEPDC1 to influence cancer progression.

The PI3K/Akt/mTOR pathway has involvement with cell proliferation, metabolism, as well as motility, which has been found to be frequently triggered in human cancer. It has been reported that DEPDC1 could activate PI3K/Akt/mTOR signaling [19], which regulates cell proliferative and migrative capabilities. It was hypothesized that the PI3K/Akt/mTOR signaling pathway may be involved in DEPDC1-mediated nephroblastoma. In the present study, markers of this signaling pathway were assessed following S100A16 knockdown. It was identified that S100A16 knockdown inhibited the phosphorylation of PI3K and Akt, as well as mTOR. However, DEPDC1 overexpression significantly reversed these effects. The in vitro assays

demonstrated that DEPDC1 promoted the tumor progression, and involved in PI3K/AKT/mTOR signaling in nephroblastoma cells.

To sum up, this study discussed the potential role that S100A16 played in nephroblastoma, the results of which provided insights into the tumor-promoting role of S100A16 in nephroblastoma cells. S100A16 could interact with DEPDC1 to promote caner progression via PI3K/AKT/mTOR axis, suggesting that it might be a promising therapeutic target and prognostic indicator of nephroblastoma. Moreover, further experiments are needed to reveal the detailed underlying mechanisms of S100A16 in nephroblastoma regulation.

Availability of data and materials

The datasets used and/or analyzed during the current study are available from the corresponding author on reasonable request.

The authors declare no conflict of interest.

References

1. Treger TD, Chowdhury T, Pritchard-Jones K, Behjati S. The genetic changes of Wilms tumour. Nat Rev Nephrol 2019; 15: 240-251.
2. Zhang J, Hou T, Qi X, et al. SOX21-AS1 is associated with clinical stage and regulates cell proliferation in nephroblastoma. Biosci Rep 2019; 39: BSR20190602.
3. Groenendijk A, Spreafico F, de Krijger RR, et al. Prognostic Factors for Wilms Tumor Recurrence: A Review of the Literature. Cancers (Basel) 2021; 13: 3142.
4. Brok J, Treger TD, Gooskens SL, van den Heuvel-Eibrink MM, Pritchard-Jones K. Biology and treatment of renal tumours in childhood. Eur J Cancer 2016; 68: 179-195.
5. Sadigh AR, Mihanfar A, Fattahi A, et al. S100 protein family and embryo implantation. J Cell Biochem 2019; 120: 19229-19244.
6. Sattar Z, Lora A, Jundi B, et al. The S100 Protein Family as Players and Therapeutic Targets in Pulmonary Diseases. Pulm Med 2021; 2021: 5488591.
7. Zhang H, Yang Y, Ma X, et al. S100A16 Regulates HeLa Cell through the Phosphatidylinositol 3 Kinase (PI3K)/AKT Signaling Pathway. Med Sci Monit 2020; 26: e919757.
8. Sun X, Wang T, Zhang C, et al. S100A16 is a prognostic marker for colorectal cancer. J Surg Oncol 2018; 117: 275-283.
9. You X, Li M, Cai H, et al. Calcium Binding Protein S100A16 Expedites Proliferation, Invasion and Epithelial-Mesenchymal Transition Process in Gastric Cancer. Front Cell Dev Biol 2021; 9: 736929.
10. Fang D, Zhang C, Xu P, et al. S100A16 promotes metastasis and progression of pancreatic cancer through FGF19-mediated AKT and ERK1/2 pathways. Cell Biol Toxicol 2021; 37: 555-571.
11. Zhu W, Xue Y, Liang C, et al. S100A16 promotes cell proliferation and metastasis via AKT and ERK cell signaling pathways in human prostate cancer. Tumour Biol 2016; 37: 12241-12250.
12. Chen D, Ito S, Hyodo T, et al. Phosphorylation of DEPDC1 at Ser110 is required to maintain centrosome organization during mitosis. Exp Cell Res 2017; 358: 101-110.
13. Kanehira M, Harada Y, Takata R, et al. Involvement of upregulation of DEPDC1 (DEP domain containing 1) in bladder carcinogenesis. Oncogene 2007; 26: 6448-6455.
14. Zhou C, Wang P, Tu M, et al. DEPDC1 promotes cell proliferation and suppresses sensitivity to chemotherapy in human hepatocellular carcinoma. Biosci Rep 2019; 39: BSR20190946.
15. Shen X, Han J. Overexpression of gene DEP domain containing 1 and its clinical prognostic significance in colorectal cancer. J Clin Lab Anal 2020; 34: e23634.
16. Zheng H, Li BH, Liu C, et al. Comprehensive Analysis of lncRNA-Mediated ceRNA Crosstalk and Identification of Prognostic Biomarkers in Wilms' Tumor. Biomed Res Int 2020; 2020: 4951692.
17. Geng G, Li Q, Guo X, et al. FOXO3a-modulated DEPDC1 promotes malignant progression of nephroblastoma via the Wnt/β-catenin signaling pathway. Mol Med Rep 2022; 26: 272.
18. Alzahrani AS. PI3K/Akt/mTOR inhibitors in cancer: At the bench and bedside. Semin Cancer Biol 2019; 59: 125-132.
19. Aoki M, Fujishita T. Oncogenic Roles of the PI3K/AKT/mTOR Axis. Curr Top Microbiol Immunol 2017; 407: 153-189.
20. Zhao H, Yu M, Sui L, et al. High Expression of DEPDC1 Promotes Malignant Phenotypes of Breast Cancer Cells and Predicts Poor Prognosis in Patients With Breast Cancer. Front Oncol 2019; 9: 262.
21. Liu L, Song Z, Gao XD, et al. Identification of the potential novel biomarkers as susceptibility gene for Wilms tumor. BMC Cancer 2021; 21: 316.
22. Høgsholt S, Asdahl PH, Bonnesen TG, et al. Disease-specific hospitalizations among 5-year survivors of Wilms tumor: A Nordic population-based cohort study. Pediatr Blood Cancer 2021; 68: e28905.
23. Domínguez B, Pardo BG, Noia M, et al. Microarray analysis of the inflammatory and immune responses in head kidney turbot leucocytes treated with resveratrol. Int Immunopharmacol 2013; 15: 588-596.
24. Babini E, Bertini I, Borsi V, et al. Structural characterization of human S100A16, a low-affinity calcium binder. J Biol Inorg Chem 2011; 16: 243-256.
25. Tu G, Gao W, Li Y, et al. Expressional and Prognostic Value of S100A16 in Pancreatic Cancer Via Integrated Bioinformatics Analyses. Front Cell Dev Biol 2021; 9: 645641.
26. Chen D, Luo L, Liang C. Aberrant S100A16 expression might be an independent prognostic indicator of unfavorable survival in non-small cell lung adenocarcinoma. PLoS One 2018; 13: e0197402.
27. Ou S, Liao Y, Shi J, et al. S100A16 suppresses the proliferation, migration and invasion of colorectal cancer cells in part via the JNK/p38 MAPK pathway. Mol Med Rep 2021; 23: 164.
28. Gong Z, Chu H, Chen J, et al. DEPDC1 upregulation promotes cell proliferation and predicts poor prognosis in patients with gastric cancer. Cancer Biomark 2021; 30: 299-307.
29. Wang W, Li A, Han X, et al. DEPDC1 up-regulates RAS expression to inhibit autophagy in lung adenocarcinoma cells. J Cell Mol Med 2020; 24: 13303-13313.
30. Tsuruta M, Ueda S, Yew PY, et al. Bladder cancer-associated cancer-testis antigen-derived long peptides encompassing both CTL and promiscuous HLA class II-restricted Th cell epitopes induced $CD4^+$ T cells expressing converged T-cell receptor genes in vitro. Oncoimmunology 2018; 7: e1415687.
31. Huang L, Chen K, Cai ZP, et al. DEPDC1 promotes cell proliferation and tumor growth via activation of E2F signaling in prostate cancer. Biochem Biophys Res Commun 2017; 490: 707-712.

Address for correspondence

Dr Ming Ming
Department of Pediatric Surgery
The Affiliated Taian City Central Hospital of Qingdao University
29 Longtan Road, Taian,
Shandong 271000, P.R. China
e-mail: mingm202208@163.com